Rare Metal Materials and Engineering
Volume 48, Issue 6, June 2019
Available online at www.rmme.ac.cn

Science Press

Cite this article as: Rare Metal Materials and Engineering, 2019, 48(6): 1742-1748.

ARTICLE

Torsional Fretting Wear of Ti6Al4V Alloys in Saline Solutions

Lin Xiuzhou[1], Cai Zhenbing[2], Yi Jinghua[2], Cui Xuejun[1], Dou Baojie[1], Zhu Minhao[2,3]

[1] Materials Corrosion and Protection Key Laboratory of Sichuan Province, Sichuan University of Science & Engineering, Zigong 643000, China; [2] Key Laboratory of Advanced Technologies of Materials, Ministry of Education, Southwest Jiaotong University, Chengdu 610031, China; [3] School of Materials Science and Engineering, Southwest Jiaotong University, Chengdu 610031, China

Abstract: Four fretting modes exist in ball-on-flat contact according to the direction of relative motion, i.e. tangential, radial, rotational, and torsional fretting. Torsional fretting in a physiological medium is one of the main reasons for artificial joints fail. A new test system was established for torsional fretting in a liquid medium at a constant temperature in a torsional mode with a ball-on-flat contact. The torsional fretting experiments were conducted using titanium alloys/zirconium dioxide ceramic balls in a saline solution at 37 °C, and the torsional fretting running behaviors and damage mechanisms were discussed. The results show that the dynamics behaviors are strongly dependent upon the torsional angular displacement amplitude and the number of cycles. A running condition fretting map (RCFM) is established, which includes 3 fretting running regimes: a partial slip regime (PSR), a mixed fretting regime (MFR), and a slip regime (SR). No damage is observed at the contact center and only slight scratch and wear are observed on the contact edge of PSR. The damage zone extends to the contact center and the sticking zone (without damage) contracts to the contact center as the number of cycles increases, and some oxidation wear and damage occur on the contact edge of MFR. The damage mechanisms are primarily abrasive wear, oxidation wear and adhesion wear in the SR.

Key words: fretting wear; torsional fretting; titanium alloy; saline solution

Titanium alloys (Ti-6Al-4V) are widely used as medical implant materials because of their excellent properties, especially for artificial joints and artificial bones[1,2]. Annually, 250 000 total hip replacements (THR) are performed in the United States. As one of the most commonly performed surgical procedures, this number is estimated to increase to 500 000 by the year 2030[3]. However, numerous studies and clinical cases have reported that 10%~20% of artificial joints need to be replaced within 15~20 years. Moreover, aseptic loosening accounts for approximately 80% of these failures[4,5].

Many scholars have studied the tribological behaviors of metallic artificial joint materials (especially titanium alloy) in open-air environments and different solutions for biomaterial applications[6,7]. Numerous scientists agree that fretting wear is a major factor in the failure of artificial joints[8-10]. Morrison[11] suggested that torsional motion is one of the most significant relative motion modes in the knee and other joints during normal walking. Therefore, it is crucial to study the torsional fretting mechanisms in terms of running motions in artificial joint materials.

According to the directions of relative motion under a contact configuration of flat-on-ball, only four basic fretting modes can be distinguished: tangential, radial, rotational and torsional fretting[12]. Torsional fretting can be defined as the relative motion induced by reciprocating torsional movement in oscillatory environments[13]. However, due to limitations in experimental equipment and conditions, only a few studies on torsional fretting have been conducted and published.

Briscoe et al[14,15] found that torsional contact is detrimental to the wear resistance of polymethyl methacrylate (PMMA), and that the interfacial energy induces a preferential debris

Received date: June 09, 2018
Foundation item: National Natural Science Foundation of China (U1633118, U1530136, 51575459); Foundation of Youth Science and Technology Innovation Team of Sichuan Province (2016TD0024, 2017TD0017); Talent Introduction Funds of the Sichuan University of Science and Engineering (2016RCL12); Open Foundation of Key Laboratory of Advanced Technologies of Materials, Ministry of Education, China
Corresponding author: Lin Xiuzhou, Ph. D., Professor, Materials Corrosion and Protection Key Laboratory of Sichuan Province, Sichuan University of Science & Engineering, Zigong 643000, P. R. China, Tel: 0086-813-5505276, Email: linxiuzhou@163.com

emission under the condition of torsional fretting. Yu et al[13] studied the torsional fretting behavior of ultra-high molecular weight polyethylene (UHMWPE), and found that torsional fretting changes from a partial slip regime (PSR) to a slip regime (SR) and the loss of material increases with increasing the torsional angular displacement. Cai et al investigated the torsional fretting friction performance of PMMA[16] and biomedical Ti6Al7Nb alloys in nitrogen ion implantations[17]. Chen et al[18] investigated the torsional fretting behavior of the head-neck interface of artificial hip joints composed of Ti6Al4V and CoCrMo alloys. Wang et al[19] designed a ball-on-socket contact configuration to simulate an artificial cervical disk, and investigated the torsional fretting wear behavior of a material combination of Ti6Al4V alloy coated by a C-DLC (carbon ion implantation-diamond like carbon) mixed layer and UHMWPE.

However, these studies on torsional fretting were all conducted in dry environments, without considering the influence of corrosive mediums. Gan et al[20] investigated torsional fretting wear behaviors of mandibular condylar cartilages in phosphate buffer saline solutions. Quan et al[21] investigated the torsional fretting behaviors of 3 kinds of porous titanium coatings in deionized water.

In this study, a new test apparatus and testing method were established for torsional fretting in solutions at constant temperatures. The torsional fretting tests were conducted on titanium alloys in saline solutions at 37 °C. The torsional fretting running behaviors and damage mechanisms of Ti6Al4V alloys under body simulation environments in vitro were discussed in detail.

1 Experiment

Ti6Al4V alloys, consisting of 6.020 wt% Al, 4.100 wt% V, 0.168 wt% Fe, 0.160 wt% O, 0.043 wt% C, and the balance Ti, are frequently used in artificial joints. As such, it was selected and machined to serve as the column specimens. Its dimensions were Φ10 mm×25 mm, with a working flat surface, which was ground and polished to a roughness (R_a) of 0.04 μm, and a diameter of 10 mm. A zirconium dioxide ceramic ball, one ceramic material commonly used in artificial joints, with a diameter of 28.575 mm, a surface roughness R_a of 0.03 μm, and a hardness of 12 000 MPa, was used as the anti-spherical specimen.

In this study, a new torsional fretting test apparatus with ball-on-flat contact was developed based on the CETR UMT-2 multifunction friction and wear tester[22, 23]. The torsional tests were conducted using normal loads (F_n) of 50, 80, and 110 N, and the corresponding maximum contact pressure in the tribo-interface was 426, 498, and 554 MPa, which do not exceed the material yield strength. The frequency (f) for most tests was 0.5, while that of others was 0.05. The angular displacement amplitudes (θ) were set as 0.2º, 0.3º, 0.5º, 1.0º, 2.0º, 3.0º, and 5.0º. The number of cycles (N) varied from 1 to 5000. The experimental medium was a saline solution with a constant controlled temperature of 37±0.5 °C.

After the torsional fretting test, the morphologies of the damaged scars were examined using an optical microscope (OM, OLYMPUS BX60MF5) and scanning electron microscopy (SEM, QUANTA2000). The chemical composition of the debris was analyzed using an energy dispersive X-ray spectroscopy (EDX, EDAX-7760/68 ME). The 2-dimensional profile of the scars was measured using a profilometer (AMBIOS XP-2).

2 Results and Discussion

2.1 Torsional fretting kinetic behavior

2.1.1 Fretting running regimes

The friction torque vs. the angular displacement amplitude loops (T_f-θ curves) can be used to characterize the torsional fretting running behaviors[16,17]. Fig.1 shows the 3-dimensional view of T_f-θ-N (Fig.1a), the surface morphology (Fig.1b), and profile (Fig.1c) of the Ti6Al4V alloy after the torsional fretting test under small angular displacement amplitudes. As shown in Fig.1a, the T_f-θ curves present a shape of line in all the cycles, which indicates that the relative motion between the contact interfaces is mainly coordinated by elastic

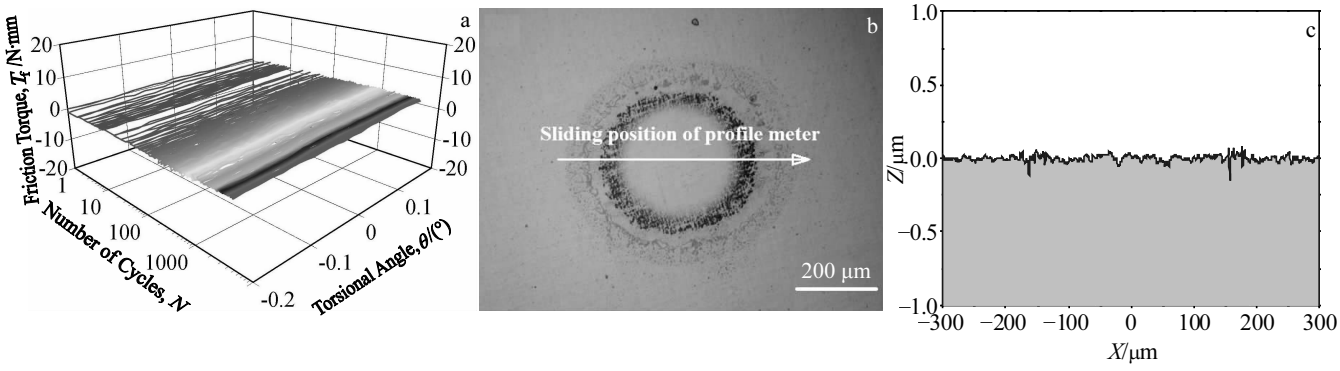

Fig.1 3-dimensional graph of T_f-θ-N (a), optical morphology (b), and the profile (c) of the damage scar of the Ti6Al4V alloy under low angular displacement amplitudes (F_n=50 N, θ=0.2°, f=0.5 Hz)

deformation. Only micro-slips occur at the contact edge, and the contact center sticks at all times. Therefore, the typical morphology of the annularity appears on the surface of the sample (Fig.1b and 1c). As such, it can be seen that fretting occurs in the partial slip regime (PSR)[16,24].

However, at large angular displacement amplitudes (such as $\theta \geq 3°$ when F_n=50 N, Fig.2a), all the T_f-θ curves are parallelograms with some waves. When introducing a torsional velocity, the waves in the T_f-θ curves disappear, and a standard parallelogram appears (Fig.3). As shown in Fig.2b and 2c, the entire contact regime is seriously damaged, and the profile appears in the shape of "U". Moreover, the sticking zone disappears, and gross slippage occurs in all the contact areas from the initiation of the torsional test (Fig.4). Therefore, the torsional fretting run occurs in the slip regime (SR) under the above conditions[16,24].

As shown in Fig.5, at intermediate angular displacement amplitudes such as 1°, the T_f-θ curves present in the shape of ellipse during most cycles. Moreover, the shape changes with increasing the cycle. After the torsional fretting test of 5000 cycles, the center of the contact region remained undamaged, and the damaged profile presented in the shape of "W" (Fig.5c). Fig.6 reveals the devolution of the damage in the first part of the test at θ=1°, and the damage scar is similar to the PSR (typical morphology of annularity). With increasing the number of cycles, the damage region extended and the adhesive region contracted to the center of the contact area, which is a typical characteristic of the mixed fretting regime (MFR) in torsional tests[16].

So, the three basic fretting regimes (PSR, MFR, and SR) can be summarized in torsional fretting experiment. In the torsional fretting experiment, for a constant angular displacement, the local motion amplitude increases from the center to the edge of the contact area. The running state in the contact area is dependent on the local motion amplitude and corresponding materials of the relative motion. When the local motion amplitude is lower than a certain value, the local region will be in a state of stick. Otherwise, it can run in a state of slip. Under different angular displacement amplitudes, the contact area in stick or slip state is different, and different evolution phenomena appear with the increase of test cycles, which leads to different damage mechanisms.

The running condition fretting map (RCFM) was established and the fretting running regimes of all the tests under various

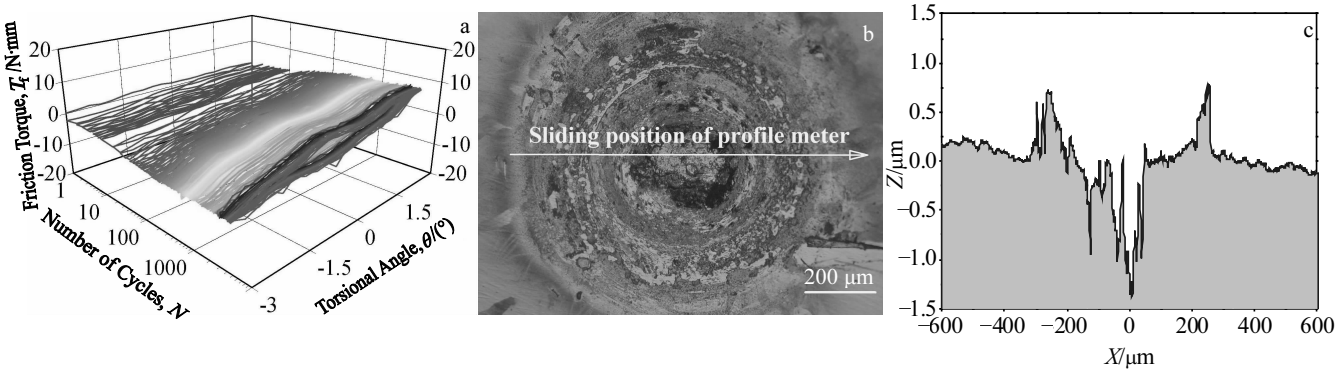

Fig.2 3-dimensional graph of T_f-θ-N (a), optical morphology (b), and profile (c) of the damage scar of the Ti6Al4V alloy under high angular displacement amplitudes (F_n=50 N, θ=3°, f=0.5 Hz)

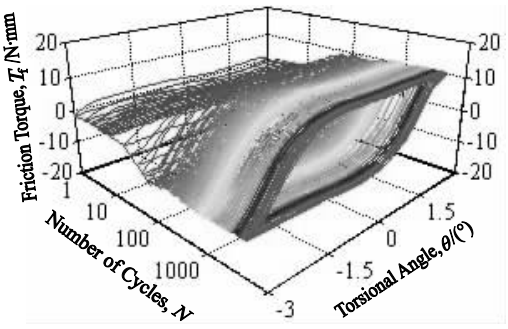

Fig.3 3-dimensional graph of T_f-θ-N for tests at low frequencies (F_n=50 N, θ=3°, f=0.05 Hz)

angular displacement amplitudes and normal loads were analyzed. As shown in Fig.7, the fretting regime varies from PSR to MFR and then to SR as angular displacement amplitudes increase. With an increase in normal loads, the width of the MFR increases, and the angular displacement amplitude at which the SR appears increases, which indicates that the relative slip between the contact interfaces becomes more difficult[25].

2.1.2 Friction torque curve

Fig.8 shows the variation in friction torque as a function of the number of cycles (T_f-N curves) under the normal load of 50 N at different angular displacement amplitudes. The T_f-N curves exhibit different characteristics in different running regimes. For instance, the friction torque in the PSR was almost constant and relatively low during the entire fretting

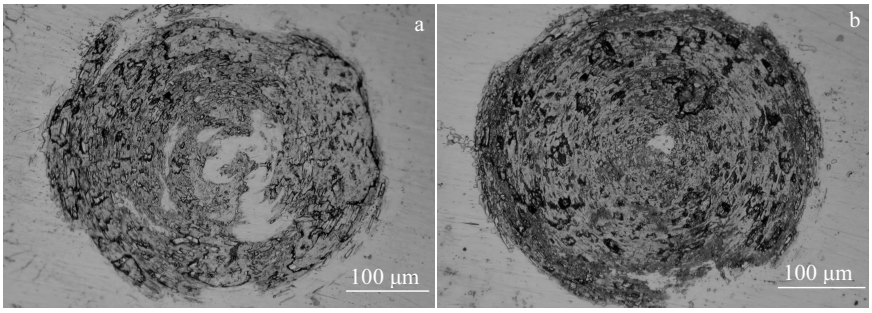

Fig.4 Optical morphologies of Ti6Al4V alloy during the first part of the torsional fretting test (F_n=50 N, θ=3°, f=0.5 Hz): (a) N=100 and (b) N=500

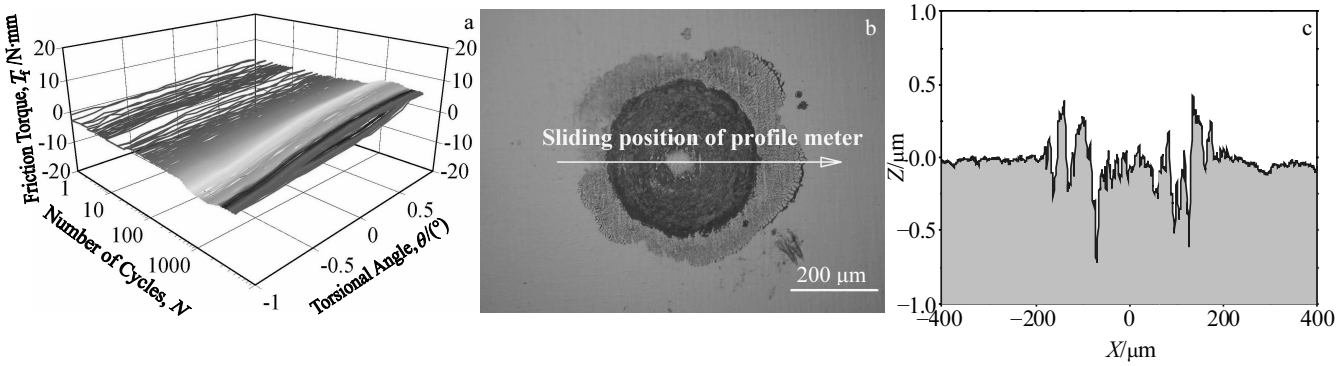

Fig.5 3-dimensional graph of T_f-θ-N (a), optical morphology (b), and profile (c) of the damage scar of the Ti6Al4V alloy under intermediate angular displacement amplitudes (F_n=50 N, θ=1°, f=0.5 Hz)

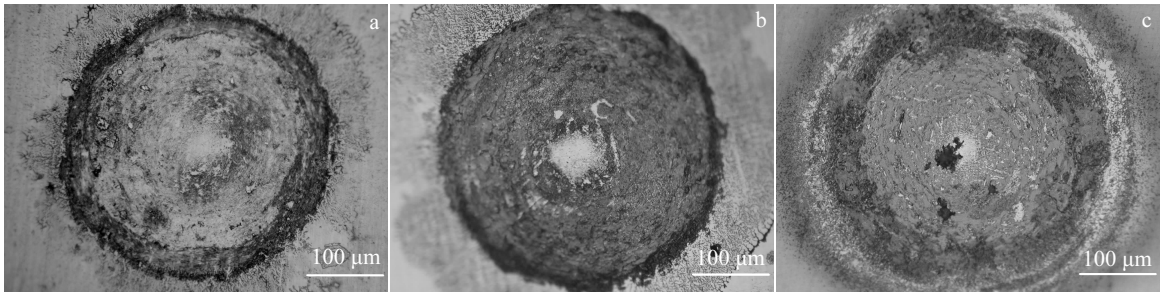

Fig.6 Optical morphologies of the Ti6Al4V alloy after the torsional fretting test with different numbers of cycles (F_n=50 N, θ=1°, f=0.5 Hz): (a) N=100, (b) N=5000, and (c) N=10 000

process (Fig.8a). As shown in Fig.8b, in the MFR, the T_f-N curves can be divided into 4 stages. In the initial stage (I), the friction torques show low levels owing to the protection and lubrication of the surface passivation films on the Ti6Al4V alloy. After 10 or tens of cycles, the curves enter the ascent stage (II), where the friction torques gradually increase as a function of the number of cycles due to the adhesion, abrasion, or plastic deformation between contact interfaces. Afterwards, the curves enter an obvious descent stage (III) for the third body bearing and lubrication function of the wear debris. Finally, the curves achieve a steady state (IV), in which the friction torque fluctuates only within a narrow range and remains stable at a relatively high level. Compared with the curves in the MFR, two obvious differences were observed in the SR (Fig.8c). First, after the ascent stage (II), decrease in the friction torque was not clear in the SR. Second, the friction torque of stage III for the SR increased greatly due to the significant wear occurring on the contact interfaces. Moreover, an obvious phenomenon can be observed, where the friction torque increases with increasing the angular displacement amplitudes and the normal loads.

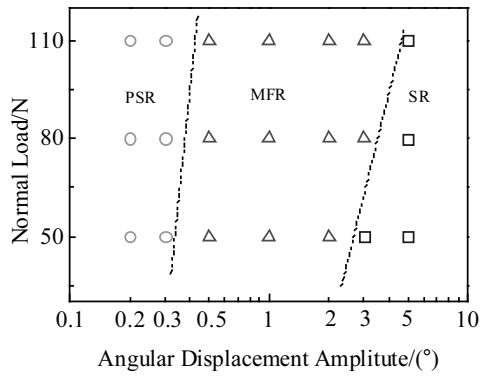

Fig.7 Running condition fretting map of the Ti6Al4V alloy in saline solution

2.2 Damage mechanisms

2.2.1 Partial slip regime (PSR)

As shown in Fig.9, some debris are displaced off the contact edge, and holes are scattered along the contact edge. Moreover, a slight detachment of particles and traces of relative sliding are also evident. Therefore, the damage of the micro-slip zone in the PSR is caused by slight abrasive wear and delamination.

2.2.2 Mixed fretting regime (MFR)

As shown in Fig.10, the original composition of the Ti6Al4V alloy is maintained in the central contact region ("A" region in Fig.10a). Some debris with different shapes (flakes in the "B" area and powder in the "C" and "D" areas in Fig.10b) were observed in the contact edge regions, and oxygen was detected in the debris. Additionally, zirconium was detected in the "B" area, which indicates that the grinding ball (zirconium dioxide) is worn and some zirconium dioxides are transferred onto the Ti6Al4V alloy surface. Therefore, the damage mechanisms in the MFR are characterized by abrasive wear and delamination, accompanied with some oxidation wear in the contact edge region.

2.2.3 Slip regime (SR)

Fig.11 and Fig.12 show the SEM micro-morphology and EDX spectrum of the damaged scar after the torsional fretting test of 5000 cycles under angular displacement amplitudes of 5° and normal load of 50 N. Increase in angular displacement amplitude gradually transforms 2-body contact into 3-body contact. Moreover, a thick debris bed (layer) formed in all the contact zones after the torsional fretting test for certain cycles in the SR.

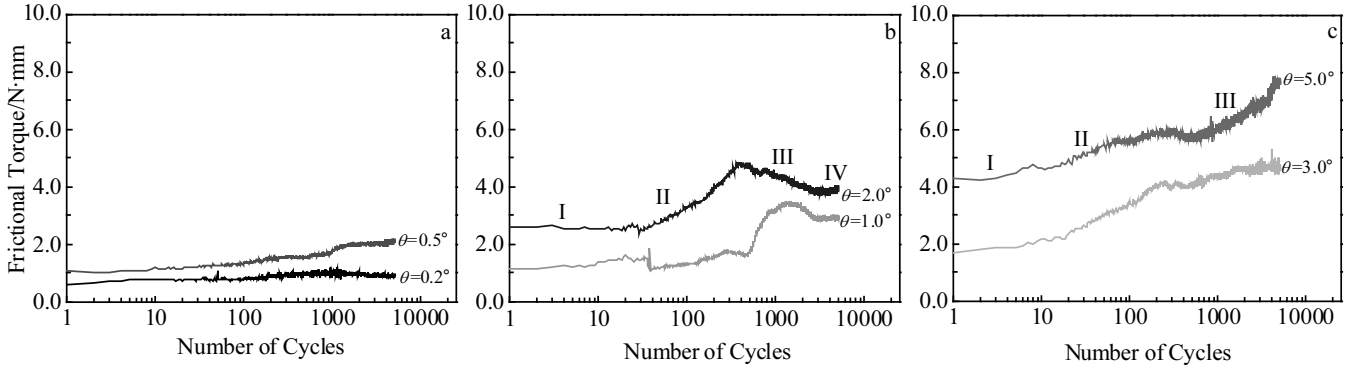

Fig.8 Friction torque curves as a function of the number of cycles in different fretting running regimes (F_n=50 N, f=0.5 Hz): (a) partial slip regime, (b) mixed regime, and (c) slip regime

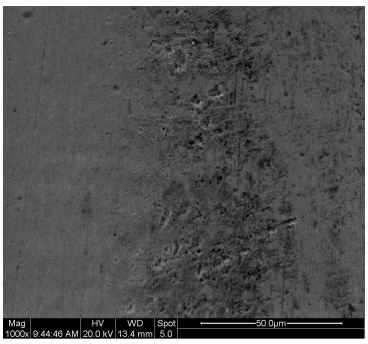

Fig.9 SEM micro-morphology in the edge region of the damage scar in the partial slip regime (F_n=50 N, θ=0.2°, f=0.5Hz, N=5000)

As shown in Fig.11, flake-shaped debris ("A" area in Fig.11a), thin powder ("C" area), and some white particles ("B" area) are evident in the central region of the damaged scar. Additionally, some delamination and plastic ploughing traces are visible on the damaged surface. Some zirconium and oxygen elements are present in the flake debris, which indicates that transfer of material from the opposite pair (zirconium dioxide ceramic ball) occurs during the test. In the "B" area shown in Fig.11a, we detected many natrium and chlorine elements using EDX. These elements were introduced through the saline solution and remained on the rough surface of the damaged scar. As shown in Fig.12, the abrasive dust is distributed along the annular edge of the damaged scar. Some oxygen elements were detected in different areas, especially along the fringe (in the "B" area).

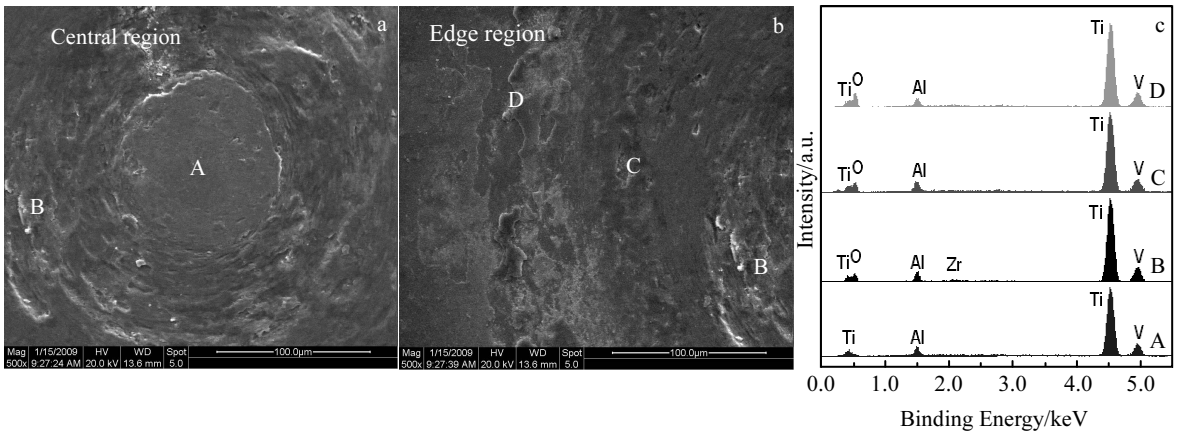

Fig.10 SEM micro-morphologies (a, b) and EDX spectra (c) of the damage scar in the mixed fretting regime (F_n=50 N, θ=2°, f=0.5 Hz, N=5000)

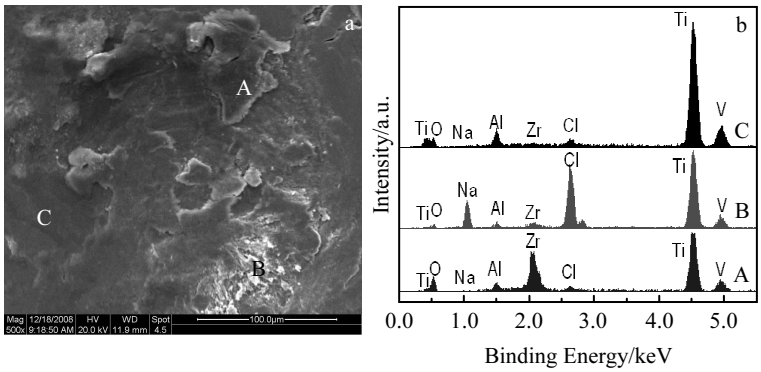

Fig.11 SEM micro-morphology (a) and EDX spectra (b) of the central region of the damaged scar in the slip regime (F_n=50 N, θ=5°, f=0.5 Hz, N=5000)

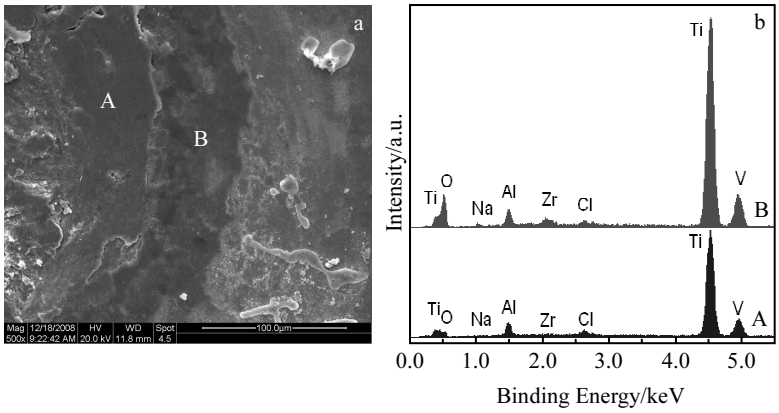

Fig.12 SEM micro-morphology (a) and EDX spectra (b) of the edge region of the damaged scar in the slip regime (F_n=50 N, θ=5°, f=0.5 Hz, N=5000)

As such, the damage mechanisms in the SR are serious abrasive wear, oxidation wear, and delamination accompanied by some material transfer.

3 Conclusions

1) The dynamic behaviors of torsional fretting of Ti6Al4V alloy are strongly dependent on the torsion angular displacement amplitudes and the number of cycles. Based on the 3-dimensional graphs of T_f-θ-N and the characteristics of the damage scars, a running condition fretting map (RCFM) is established, which includes 3 fretting running regimes: the partial slip regime (PSR), the mixed fretting regime (MFR),

and the slip regime (SR).

2) No damage is observed on the Ti6Al4V alloy contact center and only slight scratch and wear are observed on the contact edge in the PSR. The damaged zone extends to the contact center, and the sticking zone which exhibits no damage contracts to the contact center with increasing the number of cycles, and some oxidation wear and damage occur on the contact edge region in the MFR. The damage mechanisms are primarily abrasive wear, oxidation wear and adhesion wear in the SR.

References

1 Elias C N, Lima J H C, Valiev R *et al*. *JOM*[J], 2008, 60(3): 46
2 Geetha M, Singh A K, Asokamani R *et al*. *Progress in Materials Science*[J], 2009, 54(3): 397
3 Bozic K J, Kurtz S M, Lau E *et al*. *The Journal of Arthroplasty* [J], 2009, 91(1): 128
4 Pivec R, Meneghini R M, Hozack W J *et al*. *The Journal of Arthroplasty*[J], 2014, 29(1): 1
5 Katz J N, Wright E A, Polaris J J Z *et al*. *BMC Musculoskeletal Disorders*[J], 2014, 15(1): 168
6 Banchet V, Fridrici V, Abry J C *et al*. *Wear*[J], 2007, 263(7-12): 1066
7 McCann L, Udofia I, Graindorge S *et al*. *Tribology International* [J], 2008, 41(11): 1126
8 Chandra A, Ryu J J, Karra P *et al*. *Journal of the Mechanical Behavior of Biomedical Materials*[J], 2011, 4(8): 1990
9 Ryu J J, Shrotriya P. *Wear*[J], 2015, 332-333: 662
10 Dos Santos C T, Barbosa C, Monteiro M J *et al*. *Journal of the Mechanical Behavior of Biomedical Materials*[J], 2016, 62: 71
11 Morrison J B. *Journal of Biomechanics*[J], 1970, 3(1): 51
12 Zhu M H, Zhou Z R, Kapsa P *et al*. *Tribology International*[J], 2001, 34(11): 733
13 Yu J, Cai Z B, Zhu M H *et al*. *Applied Surface Science*[J], 2008, 225(2): 616
14 Briscoe B J, Chateauminois A, Lindley T C. *Tribology International*[J], 1998, 31(11): 701
15 Briscoe B J, Chateauminois A, Lindley T C. *Wear*[J], 2000, 240(1-2): 27
16 Cai Z B, Gao S S, Zhu M H *et al*. *Wear*[J], 2011, 270(3-4): 230
17 Cai Z B, Zhang G A, Zhu Y K *et al*. *Tribology International*[J], 2013, 59: 312
18 Chen K, Zhang D K, Zhang G F *et al*. *Materials and Design*[J], 2014, 56: 914
19 Wang S, Wang F, Liao Z H *et al*. *Materials Science and Engineering C*[J], 2015, 55: 22
20 Gan X Q, Cai Z B, Qiao M T *et al*. *Tribology International*[J], 2013, 63: 204
21 Quan H X, Gao S S, Zhu M H *et al*. *Tribology International*[J], 2015, 92: 29
22 Zhu M H, Lin X Z, Cai Z B *et al*. *CN Patent,* ZL200910059910.6 [P], 2011 (in Chinese)
23 Lin X Z, Cai Z B, He L P *et al*. *Journal of Southwest Jiaotong University*[J], 2011, 46(1): 132 (in Chinese)
24 Cai Z B, Zhu M H, Shen H M *et al*. *Wear*[J], 2009, 267(1-4): 330
25 Zhou Z R, Nakazawa K, Zhu M H *et al*. *Tribology International* [J], 2006, 39(10): 1068

Ti6Al4V 合金在 Saline 溶液中的扭动微动磨损

林修洲[1]，蔡振兵[2]，易敬华[2]，崔学军[1]，窦宝捷[1]，朱旻昊[2,3]

(1. 四川理工学院 材料腐蚀与防护四川省重点实验室，四川 自贡 643000)

(2. 西南交通大学 材料先进技术教育部重点实验室，四川 成都 610031)

(3. 西南交通大学 材料科学与工程学院，四川 成都 610031)

摘　要：在球/面接触中存在 4 种微动模式，即切向、径向、转动和扭动微动，在生理介质中扭动微动是人工关节失效的主要原因之一。成功建立了一种可在恒温液体介质中实现球/面接触扭动微动的新的试验系统。利用该系统，在 37 ℃的 Saline 溶液中进行了钛合金/二氧化锆陶瓷球的扭动微动试验，详细讨论了扭动微动的运行行为和损伤机理。结果表明，扭动微动动力学行为在很大程度上取决于扭动角位移振幅和周期数。研究建立了扭动微动运行工况图（RCFM），包括 3 个区域，即：部分滑移区（PSR），混合区（MFR）和完全滑移区（SR）。在部分滑移区，接触中心没有发现任何损伤，接触边缘上只观察到轻微的擦伤和磨损。在混合区，损坏区域从接触边缘向中心扩展，接触中心无损伤，接触边缘区域出现氧化磨损和损伤。在滑移区，整个接触区域均发生损伤，损伤机理主要是磨蚀磨损、氧化磨损、和粘着磨损。

关键词：微动磨损；扭动微动；钛合金；Saline 溶液

作者简介：林修洲，男，1974 年生，博士，教授，四川理工学院材料科学与工程学院，四川 成都 643000，电话：0813-5505276，E-mail: linxiuzhou@163.com